

# INITIATION OF STRESS CORROSION CRACKING IN BRASS COMPONENTS FOR DRINKING WATER SYSTEMS: SELECTED CASE STUDIES

## NAPETOSTNO KOROZIJSKO POKANJE MEDENINASTIH KOMPONENT ZA SISTEME OSKRBE S PITNO VODO: IZBRANI PRIMERI ŠTUDIJ

Mirjam Bajt Leban\*, Tadeja Kosec

Slovenian National Building and Civil Engineering Institute, Dimičeva ulica 12, 1000 Ljubljana, Slovenia

*Prejem rokopisa – received: 2026-01-14; sprejem za objavo – accepted for publication: 2026-05-07*

doi:10.17222/mit.2026.1647

Failure of various components in internal drinking-water systems leads to water leakage and high costs. Brass is an appropriate material for machining such components; however, it is sensitive to special forms of corrosion. Dezincification of duplex ( $\alpha + \beta$ ) brass can cause dealloying and cracking of components, leading to a release of lead into drinking water, which is one of the greatest health concerns for these systems. In the present study, the microstructure and fractures of three brass components that cracked after a short to moderate period of operation were investigated. The investigation showed their sensitivity to cracking regardless of the presence of a corrosive environment.

Keywords: brass, drinking water, stress corrosion cracking, dezincification, hardness

Odpoved različnih komponent v internih sistemih za oskrbo s pitno vodo povzroča iztekanje vode in visoke ekonomske stroške. Medenina je obetaven material za izdelavo takšnih komponent z mehansko obdelavo, vendar je občutljiva na posebne oblike korozije. Razcinkanje dvofazne ( $\alpha + \beta$ ) medenine lahko povzroči selektivno raztapljanje ene faze in pokanje komponent ter vodi tudi do sproščanja svinca v pitno vodo, kar predstavlja eno največjih zdravstvenih tveganj v teh sistemih. V tej študiji sta bila raziskana mikrostruktura in lom treh medeninastih komponent, na katerih so razpoke nastale kmalu čas po začetku obratovanja. Preiskava je pokazala njihovo občutljivost na različne oblike pokanja ne glede na prisotnost korozivnega okolja.

Ključne besede: medenina, pitna voda, napetostno korozijsko pokanje, razcinkanje, trdota

## 1 INTRODUCTION

Brass alloys are widely used in drinking water distribution systems due to their mechanical strength, corrosion resistance, and ease of manufacture.<sup>1</sup> Fittings, valves and connectors made from brass ensure safe and reliable water transport in residential, commercial and industrial applications. However, the long-term performance of these components is challenged by specific corrosion mechanisms that can lead to premature failure.

Stress corrosion cracking (SCC) is a critical failure mode in brass, occurring under the combined influence of tensile stresses and a corrosive environment.<sup>2-5</sup> In potable water systems, SCC can initiate from the external surface, due to atmospheric exposure and residual stresses, or from the internal surface, in contact with water whose chemistry may promote cracking. Failures caused by SCC often result in leakage within building interiors, leading to extensive water damage and significant financial losses.<sup>6</sup>

SCC susceptibility in brass can be further increased by dezincification,<sup>7-10</sup> a selective leaching process in which zinc is removed from the alloy, leaving a weakened, porous, and copper-rich structure.<sup>11</sup> Dezincification not only accelerates mechanical degradation, but can also enhance SCC initiation. Additionally, the leaching of lead,<sup>12-15</sup> which is added to brass to improve machinability,<sup>16,17</sup> rises health concerns,<sup>18,19</sup> prompting regulatory changes and the development of lead-free brass alloys.<sup>16,20,21</sup> While these new alloys offer promising solutions to lead release, their long-term SCC resistance, particularly in potable water environments, remains insufficiently understood.<sup>2,22</sup>

In this study, a comparative investigation of three different cases of failure in brass components is presented. The aim is to compare the initiation and propagation of stress-corrosion cracking (SCC) from internal and external surfaces of brass components used in drinking water systems. Visual inspection, microstructural examination and hardness measurements were conducted in order to determine the modes of cracking. Special attention is given to the influence of dezincification and alloy composition.

\*Corresponding author's e-mail:  
mirjam.bajt-leban@zag.si (Mirjam Bajt Leban)



© 2026 The Author(s). Except when otherwise noted, articles in this journal are published under the terms and conditions of the Creative Commons Attribution 4.0 International License (CC BY 4.0).

## 2 EXPERIMENTAL PART

To investigate the failure of brass components from three different buildings, designated A, B, and C, several examinations were conducted. The chemical compositions of the brass elements were analysed using optical emission spectroscopy (Spectro MAXx) and are presented in Table 1. Visual inspection of corroded and fractured surfaces was performed with a Tagarno optical microscope and a JEOL 5500 LV scanning electron microscope (SEM), equipped with Aztec Live Advanced ULTIM 65 energy-dispersive spectroscopy (EDS). Metallographic samples were prepared to examine the cross-sectional microstructures of the failed components. Microstructural observation was carried out using a Carl Zeiss Axio Imager M2m and Axio Vision software. Brinell hardness measurements of brass components that failed by SCC were performed on metallographically prepared cross-sections according to ISO 6506-1 (Metallic materials – Brinell hardness test), using a 612.9 N load and a 2.5 mm ball diameter. The hardness of individual  $\alpha$  and  $\beta$  grains was measured using the Vickers method (HV 0.005) according to ISO 6507-1 (Metallic materials – Vickers hardness test).

## 3 RESULTS

### 3.1 Description of fracture

All three failed brass components were installed in internal drinking water systems in either private or public

buildings in Slovenia, known for having drinking water that does not require additional treatment, except for occasional disinfection, for example, after emergencies such as floods or repairs of the water infrastructure. Photographs of the components in their as-received condition are presented in **Figure 1**.

**Building A:** Several connection components of hot-water system valves in an internal water supply installation failed a few months after being installed in a new building, causing a leakage.

**Building B:** In a public building, several brass press T-fittings, connecting composite pipes for cold drinking water, began to leak due to fractures after 18 years of operation. The T-fittings were installed in the cement screed on the building floor.

**Building C:** Only a few days after installation and the start of operation, an angle valve plug collapsed.

### 3.2 Fracture examination

**Brass component A:** Examination of the fractured surface of this component (**Figure 2a**) showed that the main crack originated from the pipe interior. On some of the failed elements, stepwise crack propagation is present (**Figure 2b**). The main crack surface is, based on additional EDS mapping analysis, enriched with Zn and oxygen, indicating the presence of dezincification products (**Figure 3**).

**Brass component B:** Failure of several press fittings occurred beneath the pressed section, at the transition



**Figure 1:** Failed brass components from building A (a), B (b), and C (c). The white arrow in (a) indicates the fracture of the outside thread; red arrows in (b) show the position of T-fittings inserted in the cement screed on the floor; and the yellow arrow in (c) indicates the position of the fracture at the outer thread of the plug.

**Table 1:** Chemical compositions of the investigated failed brass components given in w/%

	Cu	Zn	Pb	Sn	Ni	Al	Fe
Brass A	57.2	40.15	1.94	0.21	0.08	0.01	0.33
Brass B	55.5	39.52	2.69	1.04	0.31	0.16	0.58
Brass C	57.2	40.10	1.90	0.20	0.09	0.01	0.30
standard*	57–59	balance	1.6–2.5	0.2–0.5	< 0.3	< 0.1	< 0.4
standard**	57–59	balance	2.5–3.5	< 0.3	< 0.3	< 0.05	< 0.3

\* CW619N, SIST EN 12420

\*\* CW614N, SIST EN 12420

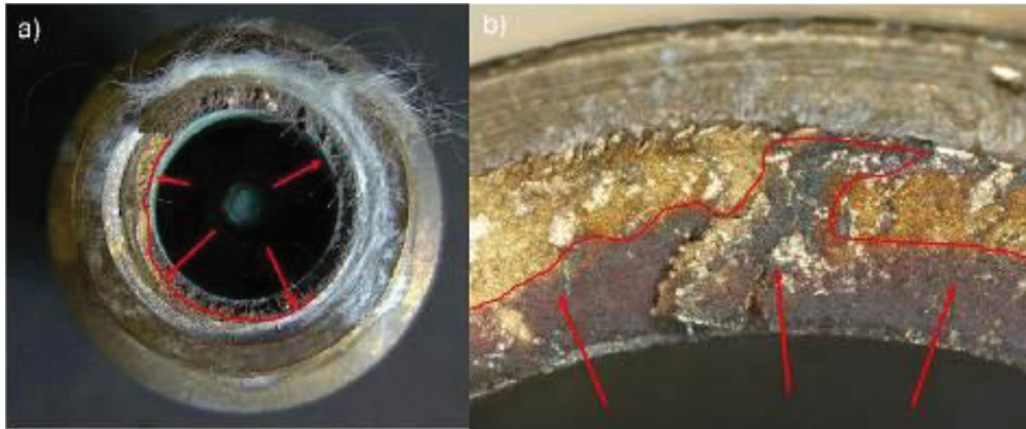


**Figure 2:** Photographs of the fractured surface of failed component A. The red line indicates the transition between SCC and ductile final fracture. The red arrows indicate the SCC mode of fracture.

from the thinnest to the thickest part (**Figure 4**). A small hole is visible in this part through which water was leaking (marked with a red arrow in **Figure 4**). After removal from the water supply system, one of the fittings was deliberately broken in the laboratory along the crack to examine the old section of the crack, which can be clearly distinguished from the fresh overload fracture. The old

fracture (**Figure 5**) consists of Cu-rich grains (identified by EDS and marked with a black arrow in **Figure 5b**) and Sn-rich cubic crystals, marked with a white arrow in **Figure 5b**. The Zn-rich phase is absent, indicating a dezincification process in which its products, unlike those in building A, were not hydrolysed, but dissolved.

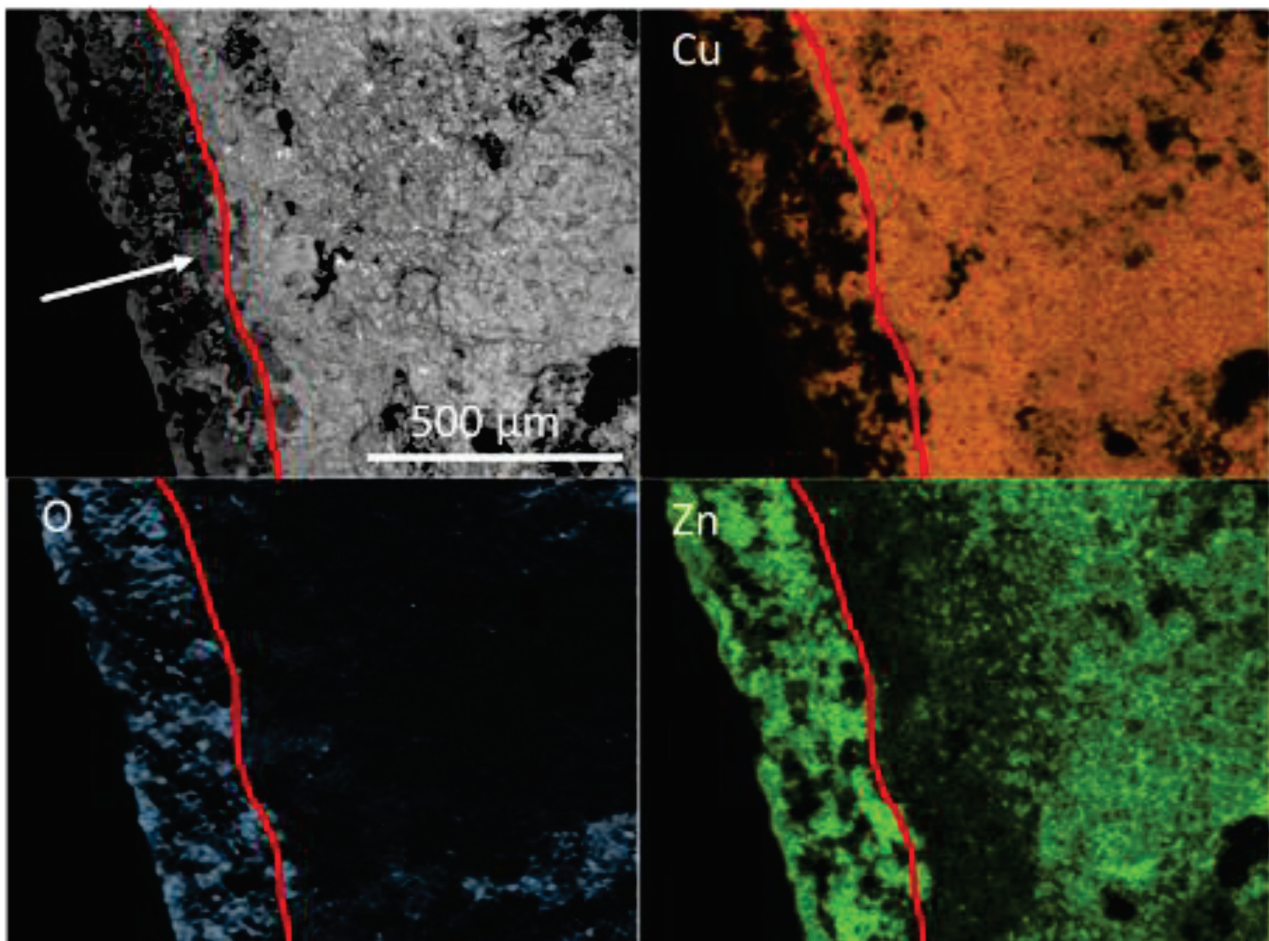


**Figure 3:** SEM-BSE (top left) and EDS mapping analysis for Cu, Zn and O of the cracked surface of specimen A

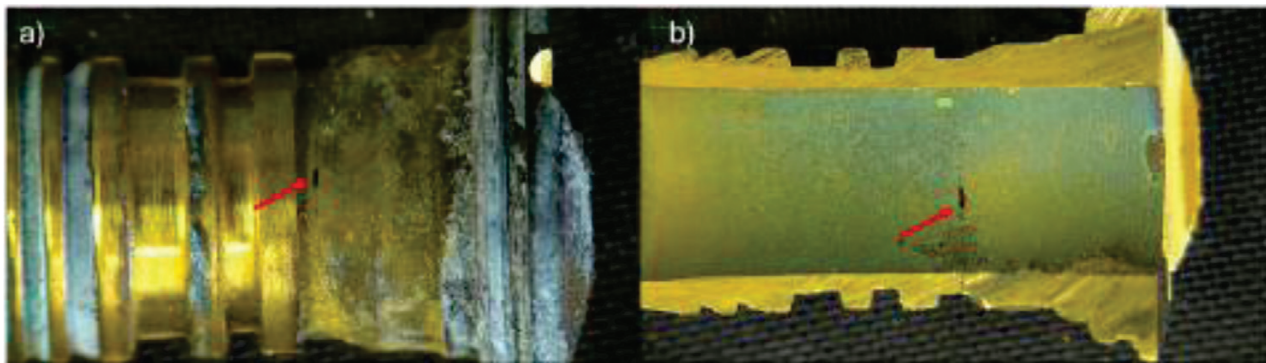


Figure 4: Press fitting (B) failure – outer surface (a) and inner surface (b). The red arrow indicates the initiation site of SCC.

Brass component C: Numerous steps are visible on the fractured surface of this element (Figure 6a). SEM analysis of the fracture revealed flat facets (Figure 6c, black arrow), probably caused by the friction between the fracture surface and the opposite side after the break, as well as intergranular corrosion between the grains present at the fracture surface, indicating the presence of intergranular corrosion (Figure 6c, white arrow).

### 3.3 Microstructural examination

Brass component A: As shown by metallographic analysis (Figure 7), the microstructure (Figure 7b) exhibits distinctly elongated  $\alpha$  grains aligned with the deformation direction, while the  $\beta'$  phase is distributed in narrow, banded regions, characteristic of cold-deformed, non-recrystallised  $\alpha + \beta'$  brass. Several cracks propagated across the cross-section of the wall of the component (Figure 7a). Stress-corrosion cracks propagated from the internal wall of the joining component towards the externally threaded brass component. The primary

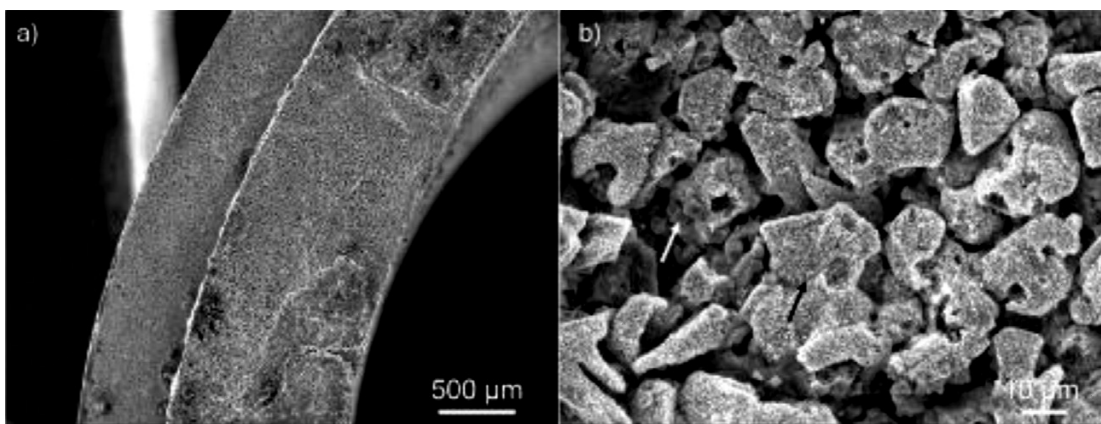


Figure 5: SEM photo of the fracture surface of press fitting B

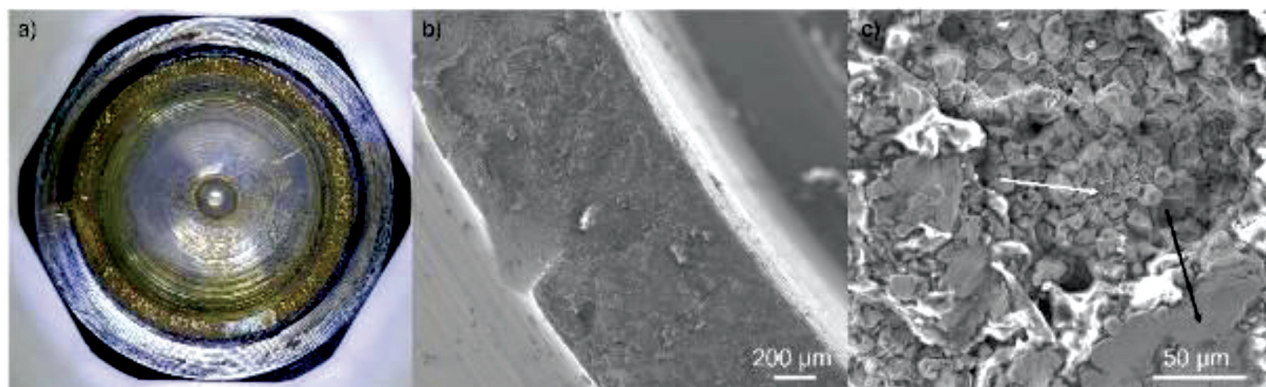
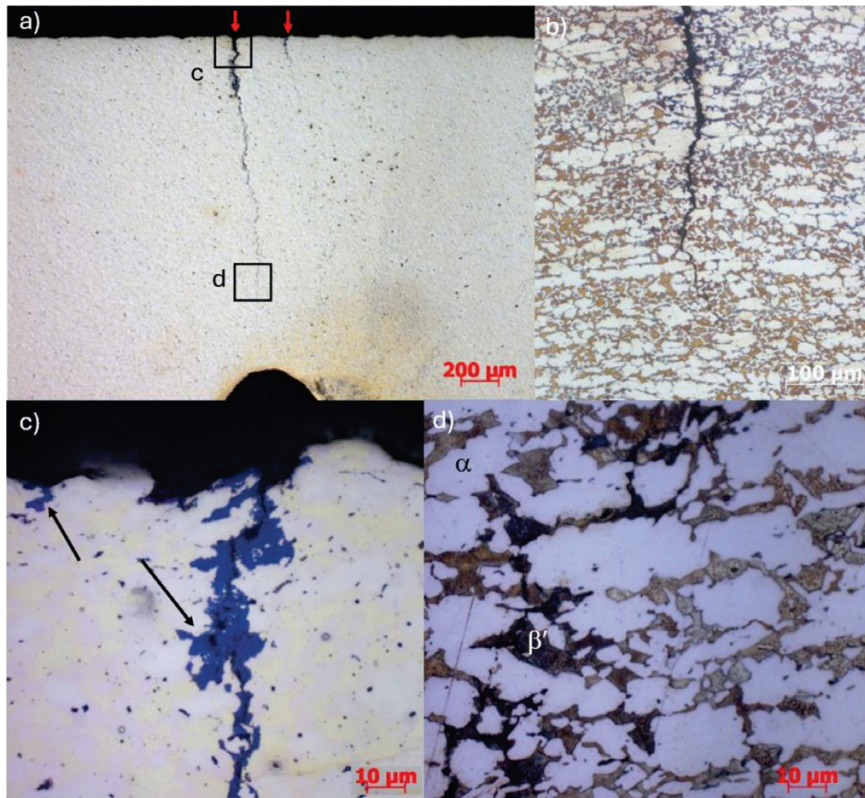


Figure 6: Fractured surface of angle valve plug with visible corrosion damage of nickel (Ni) coating at the bottom (a), and SEM images with details of the fractured surface (b and c)

crack propagation direction is in the  $\beta$ -phase, which is richer in zinc. Near the initiation site (Figure 7c), cracks are more open and the crack walls consist of a Zn-rich product; areas of dezincification are grey, similar to those described by Zhang et al.<sup>23</sup> This particular type of

corrosion was also indicated by the EDS analysis presented in Figure 3. Cracks propagate either transgranularly through  $\beta'$ -grains or intergranularly between  $\alpha$  and  $\beta'$  grains (Figure 7d).



**Figure 7:** Metallographic cross-section of a cracked site with two visible cracks in brass component A (initiation sites marked with red arrows a); microstructure near the main crack b); initiation sites of the cracks filled with grey products c); the end of the crack which propagated mainly between  $\alpha$  and  $\beta'$  phases, or through  $\beta'$  phase d)

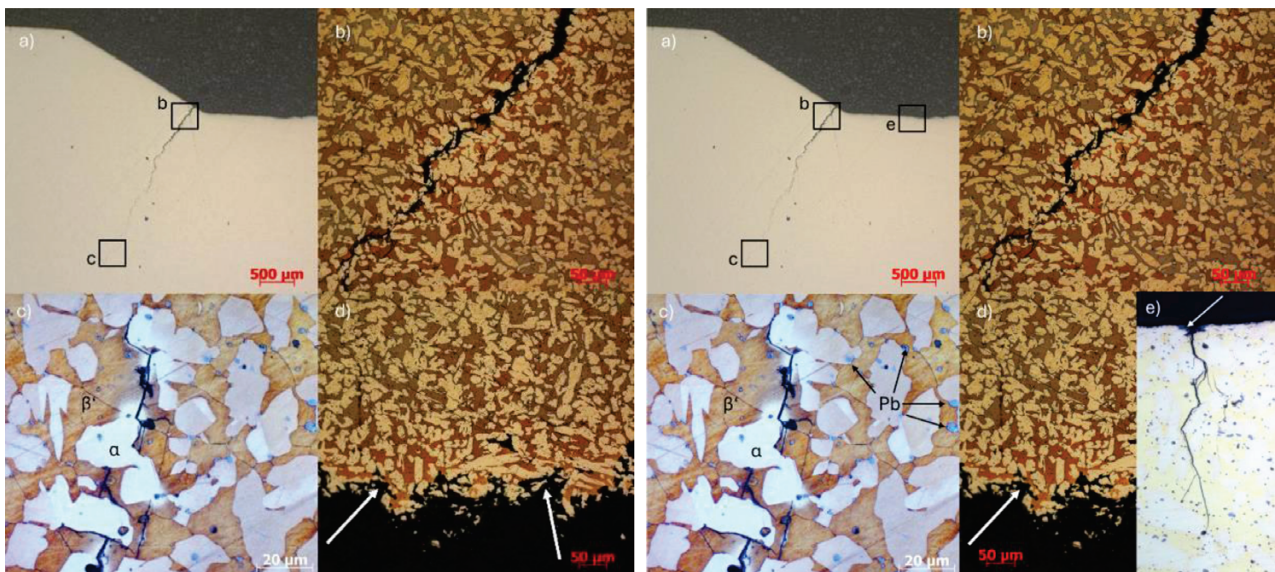


**Figure 8:** Metallographic cross-section of the cracked site, showing a visible crack initiated at the geometric transition of brass component B (a); initiation site of the crack (b); the end of the crack, which propagated mainly between the  $\alpha$  and  $\beta'$  phases or through the  $\beta'$  phase, with light grey Pb particles marked by black arrows (c); the inner side of the fitting with dezincification, marked by a white arrow (d); secondary cracks near the main fracture with a visible initiation site on Zn corrosion products (white arrow) (e).

Brass component B: As shown in **Figure 8b**, the microstructure is recrystallized, with evenly distributed  $\beta$ -phase, and rounded, polygonal  $\alpha$  grains. The crack propagated transgranularly across  $\beta'$ -grains, and also intergranularly between  $\alpha$  and  $\beta'$  grains near its end (**Figure 8c**), most likely due to cyclic bending (fatigue) of the fitting. **Figure 8d** presents a metallographic image of the inner side of the fitting, indicating that the microstructure is surface-dezincified – the  $\beta'$  phase (darker appearance) is absent from the surface, having dissolved in the water during the dezincification process. Only the  $\alpha$  phase, which is resistant to dezincification, remains at the edge.

Brass component C: The microstructure (**Figure 9b**) consists of clearly separated  $\alpha$  and  $\beta'$ -phases with relatively coarse, equiaxial grains, indicating a heat-treated (annealed) condition in the  $\alpha + \beta$  range. Two types of corrosion failures were observed: intergranular corrosion between  $\alpha$  and  $\beta'$  grains (**Figure 9b**), and corrosion under the nickel coating (**Figure 9c**). In the vicinity of both types of corrosion, Zn-rich products of grey colour are visible (**Figure 9d**).

### 3.4 Brinell hardness measurements

Brinell and Vickers hardness measurements and standard deviations for all three failed components are presented in **Table 2**.

**Table 2:** Brinell hardness measurements on failed components of the investigated elements and Vickers microhardness measurements on individual  $\alpha$  and  $\beta'$  grains

Brass component	HBW 2.5/62.5	$\alpha$ grains, HV 0.005	$\beta'$ grains, HV 0.005
A	125.3±0.5	108.0±3.3	223.7±11.6
B	112.3±3.3	139.3±9.4	219.3±40.9
C	134.7±0.9	152.0±15.6	222.3±40.5

According to the DVGW W534 technical sheet,<sup>24</sup> section 10.1.2.1., brass components resistant to stress-corrosion cracking should not have a Brinell hardness exceeding 110 HBW. These results show that a possible cause for crack formation on elements A and C could be high hardness, while the hardness of failed component B is not critically exceeded. Vickers microhardness measurements performed on individual  $\alpha$  and  $\beta'$  grains clearly show that higher hardness was measured on  $\beta'$  grains compared to  $\alpha$  grains. The  $\alpha$  grains in the heat-treated brasses (B and C) exhibit higher microhardness than in the non-heat-treated condition (A). Higher hardness of  $\alpha$  grains in heat-treated brasses can be attributed to Zn redistribution and solid-solution strengthening of the  $\alpha$  phase. In contrast, the microhardness of the  $\beta'$  phase remains essentially unchanged, reflecting its intrinsically high hardness and limited sensitivity to the applied heat treatment.<sup>24</sup>

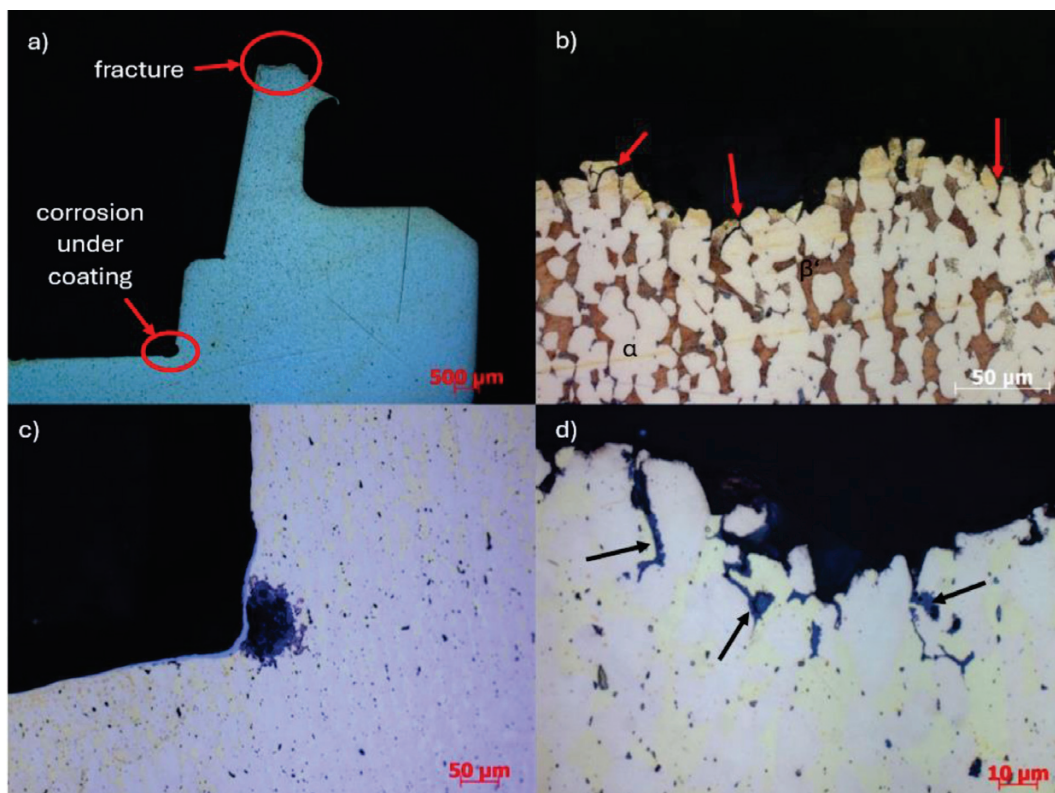


**Figure 9:** Metallographic photos of an angle valve plug a); with a visible intergranular fracture from the fractured surface – intergranular crack propagation marked with red arrows b); interior corrosion under coating c); dezincification inside intergranular corrosion, marked with black arrows d)

#### 4 DISCUSSION

All three failed components were made from similar leaded brass grades, commonly used in drinking water applications. Brass components A and B failed due to the initiation and propagation of stress corrosion cracks, while the main cause of cracking in brass component C was overload.

In the case of brass component A, cracks initiated on the inner side in contact with water and propagated through the material towards the nearest thread root. As the crack approaches the end, its branching is visible (**Figure 7c**). Similar crack propagation was observed for the failed brass component B, with the exception that the initiation site was at the outer surface, which was not in contact with drinking water (**Figure 8c**). On the other hand, in the case of the brass component A, the walls of the opened part of the crack (around 200  $\mu\text{m}$ ) were filled with grey Zn-containing products (**Figure 3**), which were not observed within the crack walls of the brass component B. However, some secondary cracks near the main crack of brass component B began to propagate from such grey products at the surface. These products consist of porous, redeposited  $\text{ZnO}/\text{Zn}(\text{OH})_2$ , formed as a result of dezincification<sup>25</sup> due to the presence of water (or high humidity) in the cementitious material, in which this component was installed. Usually, such products dissolve, leaving a Cu-rich phase; however, for the elements investigated, it is very likely that the chemical properties of the water (pH, chlorides) did not permit this.

In brass components A and B, the cracks propagated in mixed mode: either transgranularly, preferably through  $\beta'$  grains, or intergranularly between  $\alpha$  and  $\beta'$  grains. In  $\alpha+\beta'$  brasses containing approximately 40 w% Zn, the  $\beta'$  phase transforms upon cooling into an ordered  $\beta'$  structure, which adopts the B2 (CuZn-type) lattice structure.<sup>3</sup> This results in higher hardness of  $\beta'$  compared to the  $\alpha$  phase. The ordered  $\beta'$  phase exhibits stronger directional Cu–Zn bonding and fewer active slip systems than the disordered high-temperature  $\beta'$  phase, leading to limited plasticity and a tendency to cleave along specific crystallographic planes. These characteristics cause  $\beta'$  to become significantly more brittle than the  $\alpha$  phase under simultaneous mechanical and environmental loading. Consequently, stress-corrosion cracks in Cu–Zn brass of

an approximate composition Cu:Zn = 60:40<sup>4</sup> preferentially propagate transgranularly through  $\beta'$  grains.<sup>5,6</sup> This type of brass is known to be susceptible to dezincification.<sup>7–9</sup> In addition, the literature reports that brass alloys with a zinc content exceeding 15 % by weight and not additionally thermally treated tend to be susceptible to stress-corrosion cracking,<sup>3</sup> and that dezincification of brass assists SCC by increasing the stress intensity factor for crack initiation and propagation.<sup>10</sup> This might be the contributing factor accelerating SCC and explaining the short time between the start of operation and final failure of the brass component from building A. Brass component B was heat treated despite the short cracking time after the start of operation. It is therefore highly likely that the failure of brass component B was also influenced by fatigue, induced by the installation conditions. The brass component was connected to a flexible aluminium–plastic composite pipe which was not rigidly fixed to the supporting structure; consequently, pressure fluctuations in the water system allowed slight movements of the pipe, leading to cyclic loading and fatigue of the brass component.

Based on the investigational evidence, the contribution of corrosion to the final failure of brass component C is considered negligible. The failure is therefore attributed primarily to mechanical overloading during installation. Compared to brass components A and B, component C exhibits higher hardness, which is associated with reduced ductility and an increased susceptibility to cracking.<sup>26</sup> However, once the crack formed, intergranular corrosion and selective dissolution of the  $\beta'$  phase occurred, as can be seen in **Figure 9b**. SEM analysis of the cracked surfaces B and C revealed that after the formation of cracks, their surfaces began to corrode selectively – the  $\beta'$  phase dissolved, while the  $\alpha$  phase remained intact (see **Figure 5b** of the B crack surface and **Figure 6c** for the C surface). Interestingly, the B crack surface also showed intergranular corrosion, even though the crack had progressed from the outside area, which was not in contact with drinking water. In this case, due to numerous previously cracked identical elements in the building, the entire area, in which they were installed, was soaked with drinking water, causing the observed corrosion. This was not observed for component A, whose crack surfaces were covered by Zn-containing products.

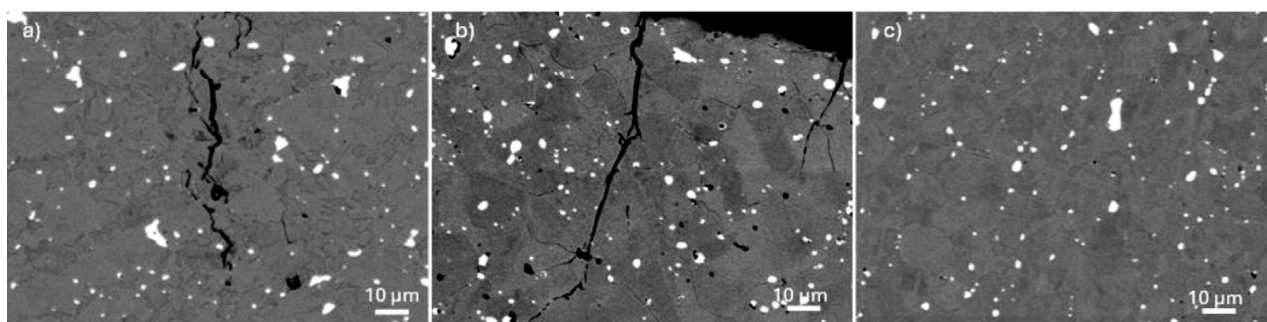


**Figure 10:** Backscattered electron images of the investigated brass components A (a), B (b), C (c). Pb particles are white in all images.

However, a detailed view of the cross-section of the crack in this component near its initiation (**Figure 7b**) reveals selective corrosion of the  $\beta'$  phase.

According to the literature<sup>2</sup>, coarsened lead particles in brass can increase internal stresses and promote SCC. The amounts, shapes, and distribution levels of Pb in the investigated cases were similar (**Figure 10**). Only in the case of brass component A, in addition to round particles, there were also coarser particles of irregular shapes. However, no correlation between crack initiation or propagation and such Pb particles was observed.

Chemical composition of water and its physical and chemical properties (conductivity, pH, chloride level, hardness, carbonates, alkalinity, etc.) strongly influence degradation of brass.<sup>27</sup> The water composition of none of the investigated components in this study was known and its effect was not studied. As reported in the literature,<sup>7</sup> a wide pH range and chloride content can lead to dezincification and may also promote stress-corrosion cracking.

## 5 CONCLUSIONS

Based on the investigation of three different brass components installed at different locations in contact with drinking water, the following conclusions can be drawn:

- The main cause of failure for all three components was cracking: stress corrosion cracking for components A and B, and overloading for component C.
- Stress corrosion cracks propagated in a mixed mode, including transgranular and intergranular propagation.
- At the fractured surfaces, evidence of either preferential dissolution of the  $\beta'$  phase, intergranular corrosion, or both is present.
- Elevated hardness, as an additional factor increasing susceptibility to stress corrosion cracking, could have contributed to this process only in the case of component A.
- Duplex brass is prone to delayed fracture due to overloads.
- No correlation between stress corrosion cracking initiation or propagation and Pb particle size, shape, and position within  $\alpha$  and  $\beta'$  grains was observed.

## 6 REFERENCES

- <sup>1</sup> M. Schütze, R. Feser, R. Bender, Corrosion resistance of copper and copper alloys: corrosive agents and their interaction with copper and copper alloys, DEHEMA: Wiley-VCH, Germany, Frankfurt am Main 2011
- <sup>2</sup> H. Wang, C. Ji, Z. Song, et al., The effect of lead content on stress corrosion behavior of brass, *Corros. Sci.*, 245 (2025), 112714, doi:10.1016/j.corsci.2025.112714
- <sup>3</sup> J. Johansson, V. Bushlya, C. Obitz, et al., Influence of sub-surface deformation induced by machining on stress corrosion cracking in lead-free brass, *Int. J. Adv. Manuf. Technol.*, 122 (2022), 3171–3181, doi:10.1007/s00170-022-10081-x
- <sup>4</sup> C. M. Giordano, G. S. Duffó, J. R. Galvele, The effect of Cu<sup>2+</sup> concentration on the stress corrosion cracking susceptibility of  $\alpha$ -brass in cupric nitrate solutions, *Corros. Sci.*, 39 (1997), 1915–1923, doi:10.1016/S0010-938X(97)00085-1
- <sup>5</sup> J. R. Galvele, Surface mobility mechanism of stress-corrosion cracking, *Corros. Sci.*, 35 (1993), 419–434, doi:10.1016/0010-938X(93)90175-G
- <sup>6</sup> D. Grice, B. Sorenson, Product Liability Case Study: Failure of Brass Plumbing Fitting due to Stress Corrosion Cracking, *AM&P Technical Articles*, 183 (2025), 21–25, doi:10.31399/asm.amp.2025-07.p021
- <sup>7</sup> M. Bajt Leban, Tadeja Kosec, Andraž Legat, Dezincification of brass in drinking water of higher hardness and lower chloride concentration, In: *Proceedings of CEOCOR 2016*, 7
- <sup>8</sup> S. Berndorf, A. Markelov, S. Guk, et al., Development of a Dezincification-Free Alloy System for the Manufacturing of Brass Instruments, *Metals*, 14 (2024), 800, doi:10.3390/met14070800
- <sup>9</sup> M. Latva, T. Kaunisto, A. Pelto-Huikko, Durability of the non-dezincification resistant CuZn40Pb2 brass in Scandinavian waters, *Eng. Fail. Anal.*, 74 (2017), 133–141, doi:10.1016/j.engfailanal.2017.01.011
- <sup>10</sup> A. Pelto-Huikko, N. Salonen, M. Latva, Dezincification of faucets with different brass alloys, *Eng. Fail. Anal.*, 169 (2025), 109202, doi:10.1016/j.engfailanal.2024.109202
- <sup>11</sup> E. Sarver, Y. Zhang, M. Edwards, Review of Brass Dezincification Corrosion in Potable Water Systems, *Corros. Rev.*, 28 (2010), 155–196, doi:10.1515/CORRREV.2010.28.3-4.155
- <sup>12</sup> Y. Zhang, M. Edwards, Zinc content in brass and its influence on lead leaching, *J. AWWA*, 103 (2011), 76–83, doi:10.1002/j.1551-8833.2011.tb11496.x
- <sup>13</sup> S. Gonzalez, R. Lopez-Roldan, J.-L. Cortina, Presence of metals in drinking water distribution networks due to pipe material leaching: a review, *Toxicol. Environ. Chem.*, 95 (2013), 870–889, doi:10.1080/02772248.2013.840372
- <sup>14</sup> K. J. Pieper, R. Martin, M. Tang, et al., Evaluating Water Lead Levels during the Flint Water Crisis, *Environ. Sci. Technol.*, 52 (2018), 8124–8132, doi:10.1021/acs.est.8b00791
- <sup>15</sup> K. J. Pieper, L.-A. H. Krometis, D. L. Gallagher, et al., Incidence of waterborne lead in private drinking water systems in Virginia, *J. Water Health*, 13 (2015), 897–908, doi:10.2166/wh.2015.275
- <sup>16</sup> J. Johansson, P. Alm, R. M'Saoubi, et al., On the function of lead (Pb) in machining brass alloys, *Int. J. Adv. Manuf. Technol.*, 120 (2022), 7263–7275, doi:10.1007/s00170-022-09205-0
- <sup>17</sup> J. Johansson, H. Persson, J.-E. Ståhl, et al., Machinability Evaluation of Low-Lead Brass Alloys, *Procedia Manuf.*, 38 (2019), 1723–1730, doi:10.1016/j.promfg.2020.01.102
- <sup>18</sup> Guidelines for drinking-water quality: fourth edition incorporating the first and second addenda, <https://www.who.int/publications/i/item/9789240045064>, Accessed 4 Dec 2025
- <sup>19</sup> Lead in drinking-water: Health risks, monitoring and corrective actions, <https://www.who.int/publications-detail-redirect/9789240020863>, Accessed 17 Apr 2024
- <sup>20</sup> A. Naza, Corrosion behavior of lead-free and dezincification resistant brass alloys in tap water (dissertation), KTH, Stockholm 2021, Retrieved from <https://urn.kb.se/resolve?urn=urn:nbn:se:kth:diva-299738>
- <sup>21</sup> K. Saber, A. Ouedrhiri, F. Hamouche, et al., Study of the Corrosivity of Two Lead-Free Brass Alloys Used in Drinking Water Supply Pipes in an Aggressive Soil, *J. Bio-Tribo-Corros.*, 11 (2025), 78, doi:10.1007/s40735-025-01003-x
- <sup>22</sup> J. Choucri, A. Balbo, F. Zanotto, et al., Corrosion Behavior and Susceptibility to Stress Corrosion Cracking of Leaded and Lead-Free Brasses in Simulated Drinking Water, *Materials*, 15 (2021), 144, doi:10.3390/ma15010144
- <sup>23</sup> Y. Zhang, Dezincification and Brass Lead Leaching in Premise Plumbing Systems: Effects of Alloy, Physical Conditions and Water Chemistry. Virginia Tech, 2009

- <sup>24</sup> J. R. Davis, *Alloying: Understanding the Basics*, ASM International, 2001, doi:10.31399/asm.tb.aub.9781627082976
- <sup>25</sup> S.-J. Chao, M.-H. Tsai, R.-P. Yu, et al., Dezincification of brass water meters in a long-term study: effects of anions, alkalinity, and residual chlorine, *Environ. Sci. Water Res. Technol.*, 7 (2021), 1666–1676, doi:10.1039/D1EW00351H
- <sup>26</sup> P. E. Schweitzer, A. Philip, *Fundamentals of Metallic Corrosion: Atmospheric and Media Corrosion of Metals*, 1st ed., CRC Press, 2006, doi:10.1201/9780849382444
- <sup>27</sup> R. Pascual, C. Bagnall, Cracking of brass fittings in water distribution systems, (2014) <https://www.gruppofrattura.it/ocs/index.php/esis/ECF18/paper/view/6076/1961>